J For Res (2015) 20:85–93
DOI 10.1007/s10310-014-0463-0

ORIGINAL ARTICLE

Variation in sap flux density and its effect on stand transpiration estimates of Korean pine stands

Minkyu Moon · Taekyu Kim · Juhan Park · Sungsik Cho · Daun Ryu · Hyun Seok Kim

Received: 21 May 2014 / Accepted: 14 August 2014 / Published online: 12 September 2014

Abstract Accurate estimates of stand transpiration (E) require the consideration of three types of variation in sap flux density (J_S): radial, azimuthal, and tree-to-tree variation. In this study, the J_S variation of 50-year-old Korean pine (*Pinus koraiensis*) trees and its effect on E estimates was evaluated using Granier-type heat dissipation sensors. The value of J_S decreased exponentially with the radial depth from cambium to pith, and the coefficient of variation (CV) for radial variation was 124.3 %. Regarding the azimuthal variation, the value of J_S differed significantly among aspects and the average CV was 23.6 %. The average CV for tree-to-tree variation was 34.0 %, and the daily CV increased with increasing vapor pressure deficit (D). The error in the E estimates caused by ignoring the radial variation was the largest (109.2 %), followed by those caused by ignoring the tree-to-tree and azimuthal variations (24.3 and 12.6 %, respectively). While the contribution of the azimuthal variation to the E estimates was minimal in comparison to the other variations, the azimuthal variation among aspects was significant, and the usage of the north aspect measurement did not generate substantial error in the E estimates (0.6 %). Our results suggest that the variation, particularly the species- and site-specific radial variation, must be considered when accurately calculating E estimates.

Keywords Azimuthal variation · Radial variation · Sap flux · Stand transpiration · Tree-to-tree variation

M. Moon · J. Park · S. Cho · D. Ryu · H. S. Kim (✉)
Department of Forest Sciences, Seoul National University, 1 Gwanak-ro, Gwanak-gu, Seoul 151-921, Republic of Korea
e-mail: hyunskim70@gmail.com

T. Kim
National Institute of Environmental Research, 42 Hwangyong-ro, Seo-gu, Incheon 404-780, Republic of Korea

H. S. Kim
National Center for Agro Meteorology, 1 Gwanak-ro, Gwanak-gu, Seoul 151-744, Republic of Korea

H. S. Kim
Research Institute for Agriculture and Life Sciences, 1 Gwanak-ro, Gwanak-gu, Seoul 151-921, Republic of Korea

Introduction

The transpiration rates of individual trees are commonly measured with various types of sap flux density (J_S) sensors [e.g., heat dissipation (Granier 1985), heat field deformation (Jiménez et al. 2000), and heat pulse velocity (Hatton et al. 1995)], and this tree-level estimation is subsequently scaled up to stand- or catchment-level transpiration. Sap flux sensors are particularly useful in complex terrain such as mountain regions, where they are employed in conjunction with data loggers to store continuously measured data (Granier et al. 1996; Köstner et al. 1998; Wilson et al. 2001; Kubota et al. 2005; Kume et al. 2010b).

However, the spatial variation of J_S within or among trees complicates the scaling from point measurements to tree- or stand-level transpiration rates (Phillips et al. 1996; Cermak and Nadezhdina 1998; Oren et al. 1998; Wilson et al. 2001; Ford et al. 2007; Tateishi et al. 2008; Kume et al. 2010a; 2012; Paudel et al. 2013), as the J_S sensor captures only a trivial proportion of the spatial variation in J_S throughout the entire xylem (Clearwater et al. 1999; Kumagai et al. 2005; Gebauer et al. 2008; Caylor and Dragoni 2009; Kume et al. 2010b; Barij et al. 2011; Alvarado-Barrientos et al. 2013; Paudel et al. 2013; Shinohara et al. 2013; Chang et al. 2014). Therefore, a

large error may be introduced when J_S is scaled from a single point measurement to the whole tree without consideration of its spatial variation; that is, its radial, azimuthal, and tree-to-tree variations, which represent the J_S variation with xylem radial depth from the cambium, around the stem, and among trees within a stand, respectively.

Regarding radial variation, J_S normally decreases with radial depth from the cambium, especially in coniferous species (e.g., Phillips et al. 1996; Ford et al. 2004b; Fiora and Cescatti 2006). However, the radial profile of J_S differs between species and even among individual trees of the same species, and ignoring this variation can cause errors of up to 300 % in E estimates (Nadezhdina et al. 2002; Čermák et al. 2004; Kume et al. 2010b). Although azimuthal variation is commonly minimal compared to other variations, failing to consider it can also cause significant errors in E estimates. Tateishi et al. (2008) and Tsuruta et al. (2010) reported that the errors due to ignoring azimuthal variation reached 20 % in *Quercus glauca* and 30 % in *Chamaecyparis obtuse* based on tree-level estimation. Nevertheless, many studies still use one-directional measurement, usually of the north aspect, based on the assumption that azimuthal variation is trivial when a large number of sensors are used for scaling to the tree or stand level (e.g., Wilson et al. 2001; Poyatos et al. 2007; Alvarado-Barrientos et al. 2013). Finally, tree-to-tree variation is another key factor in accurate E estimates, as tree-to-tree variation within the same stand and species can vary considerably; therefore, disregarding tree-to-tree variation can also cause significant error in E estimates (Delzon et al. 2004; Kumagai et al. 2005; Kume et al. 2010b; Kume et al. 2012; Shinohara et al. 2013).

As mentioned above, the variation in J_S consists of several different variations (i.e., the radial, azimuthal, and tree-to-tree variations). However, several studies have examined these separate components of the variation in J_S in order to compare their impacts on E estimates in tree stands (e.g., Kume et al. 2012; Shinohara et al. 2013). Kume et al. (2012) reported that the errors caused by azimuthal variation (16. and 21.6 %) were smaller than the errors caused by radial (33 and 44 %) and tree-to-tree (50 and 52 %) variations in *Robinia pseudoacacia* and *Quercus liaotungensis*, respectively. Shinohara et al. (2013), who studied a *Cryptomeria japonica* plantation, reported that the error caused by radial variation (15.1 %) was smaller than the errors caused by azimuthal and tree-to-tree variations (16.1 and 18.9 %, respectively).

Although these studies quantified the various variations and compared their effects on E estimates, their relative importance to E estimates was rather species- and site-dependent. Thus, these results have limited application for accurately estimating E in other species or sites. Therefore, in the present study, we evaluated the radial, azimuthal, and tree-to-tree variations in J_S for 50-year-old Korean pine trees in a plantation to obtain accurate E estimates using a heat dissipation sensor designed by Granier (1985). The purposes of the study were to (1) determine the levels of the three different types of J_S variation and (2) calculate the errors in E estimates when these spatial variations were not considered.

Materials and methods

Site description

Our study was conducted at a Korean pine plantation. This plantation was established approximately 180 m above sea level in 1963 at Mt. Taehwa, GyeongGi (37°18′15″N, 127°19′00″E). In this area, the average air temperature is 11.5 °C, and the average precipitation is 1,471 mm. The bedrock of Mt. Taehwa is primarily composed of granite. Subcanopy species in the plantation include *Toxicodendron trichocarpum*, *Rhododendron yedoense*, *Magnolia kobus*, and *Zanthoxylum schinifolium*, and the average tree density and canopy height are approximately 450 tree ha^{-1} and 18 m, respectively. The leaf area index (LAI) was developed from a site- and species-specific allometric equation by Ryu et al. (2014). The maximum and the minimum LAI during the growing season are approximately 5.40 m^2 m^{-2}, around early September, and 3.81 m^2 m^{-2}, around late March, respectively.

A study plot of 20 × 20 m for measuring radial and tree-to-tree variations was established in the plantation facing the northeast side in April 2011, and the slope angle is approximately 10°. Three trees located within 80 m of the plot were added for measurements of azimuthal variation in March 2012. These three trees were located within 10 m of each other.

Meteorological factors were measured at a tower located at the center of the plot. The air temperature (T) and relative humidity (RH) (HMP35C, Campbell Scientific, Logan, UT, USA), as well as the photosynthetically active radiation (Q, LI-190, LI-COR, Lincoln, NE, USA), were measured at the top of a tower 20 m high. These sensors were positioned slightly higher than the canopy height. The vapor pressure deficit (D) was calculated using T and RH. All of the measurements were taken every 30 s, and the 30 min average was stored on a data logger (CR1000, Campbell Scientific). Table 1 shows the meteorological variables during the study periods.

Sap flux density measurement

Granier-type heat dissipation sensors (Granier 1985; Granier 1987) were used for the J_S measurements. Each sensor

Table 1 Meteorological variables (T daily average air temperature, Q daily average photosynthetically active radiation, D daily average vapor pressure deficit)

Period	T (°C)	Q (μmol m^{-2} s^{-1})	D (kPa)
May 26–June 4, 2011	18.6 (15.9–21.8)	398 (189–609)	0.76 (0.18–1.47)
May 5–14, 2012	15.7 (12.8–17.0)	420 (79–584)	0.98 (0.20–1.57)

The *numbers in parentheses* represent the range of each variable for the given period

was composed of two different probes: an upper probe heated by a constant power (0.2 W) and a lower reference probe. The two probes were inserted radially into the stem at breast height and parted vertically from 13 to 15 cm to avoid thermal interference between them. The temperature difference between the probes was measured and converted into J_S as described by Granier (1987). Measurements were taken every 30 s, and the 30-min averages were stored in the data logger (CR1000, Campbell Scientific).

The study plot contained twenty Korean pine trees. We used four of these trees to assess radial variation. Three J_S sensors were installed in each tree at different depths from the cambium to cover 0–60 mm of the xylem ($J_{S\_0–20}$, $J_{S\_20–40}$, and $J_{S\_40–60}$, respectively). The outer sensors were installed at the north aspect to avoid direct radiation, and the $J_{S\_20–40}$ and $J_{S\_40–60}$ sensors were installed approximately 15 cm apart from the outer sensor to prevent thermal interference. To evaluate the azimuthal variation, six J_S sensors were installed at six aspects around the stem for each tree. All of the installed sensors were outer sensors, and each sensor was separated by 60°, starting from the north aspect. To gauge the tree-to-tree variation, fourteen outer sensors installed at fourteen trees in the plot were used for analysis. Table 2 shows the details of the studied trees, sensor installation, and measurement periods.

Stand transpiration calculation and error quantification

To quantify the errors in the E estimates caused by the radial, azimuthal, and tree-to-tree variations, we compared the reference E (E_R) estimates with estimates in which we ignored each source of variation. The E_R was calculated using 10 days of J_S data (i.e., March 26–June 4, 2011) from all of the outer sensors of the fourteen trees. First, the individual tree transpiration (E_T) was calculated as follows:

$$E_T = \sum_{i=1}^{n} J_{S\_A\_i} A_i, \quad (1)$$

where n is the number of the sapflux sensor depth along the xylem, A_i is the xylem area at depth i, and $J_{S\_A\_i}$ is the weighted J_S accounting for azimuthal variation. The

Table 2 Details of study trees, sensor installation, measurement periods, and the coefficient of variation (CV) for each variation type

Variations	No. of trees	Depth (mm) and aspect	DBH (cm)	Data periods	CV (%)
Radial	4	0–20, 20–40 and 40–60 at N	28.0 (21.7–31.7)	May 26–June 4, 2011	124.3
Azimuthal	3	N, NE, SE, S, SW and NW at 0–20	30.4 (26.0–36.8)	May 5–May 14, 2012	23.6
Tree-to-tree	14	0–20 at N	29.1 (21.5–36.4)	May 26–June 4, 2011	34.0

Sensors were installed at 0–20, 20–40, and 40–60 mm from the cambium

N, NE, SE, S, SW, and NW represent the aspects of the circumferentially installed sensors, and the sensors were sequentially installed 60° apart starting from the north aspect (*N* north, *NE* northeast, *SE* southeast, *S* south, *SW* southwest, *NW* northwest)

The average tree diameter at breast height (DBH) and its range are also represented for each variation type

sapwood depth was determined from the point where J_S reaches zero instead of from color distinction (e.g., Shinohara et al. 2013) or xylem water content (e.g., Fiora and Cescatti 2006). Similar to many studies which have claimed a discrepancy between the entire sapwood area and the hydroactive sapwood area (e.g., Cermak and Nadezhdina 1998; Poyatos et al. 2007), our study trees showed no clear distinction between sapwood and heartwood by color, and only a small part in the center of the xylem differed from the other part by color (Fig. 1). Therefore, in this study, we calculated E based on the assumption that the sapwood depth was the point at which J_S reaches zero. To assess the azimuthal variation of these trees, we assumed that all fourteen trees had the same average azimuthal variation as the three trees for which we measured the azimuthal variation (Kume et al. 2012; Shinohara et al. 2013). The radial variation was also evaluated using the average J_S ratios across the different depths observed in this study. In addition, we assumed that the J_S for parts of the xylem >60 mm from the cambium could be ignored, as these values were almost zero. Six of the twenty trees were not measured but were also accounted for in a similar way by assuming average outer J_S and ratio values for the radial and azimuthal variations. Consequently, the E_R was calculated using the following equation: $E_R = \sum E_T / A_G$, where A_G is the study plot area.

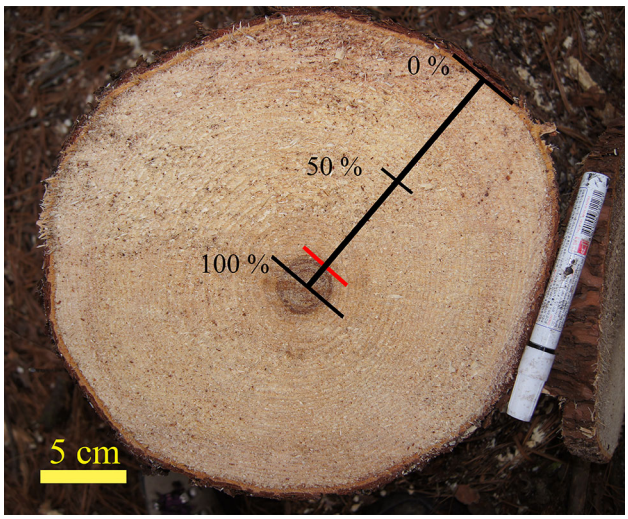

Fig. 1 A cross-section of a Korean pine tree in Mt. Taehwa, Korea. *Black bars* mark various relative depths from the cambium, while the *red bar* represents the boundary line based on color distinction

Similar to the methods employed by Kume et al. (2012) and Shinohara et al. (2013), the E estimates that did not consider the radial variation were calculated assuming that the inner J_S values ($J_{S\_20–40}$ and $J_{S\_40–60}$) were the same as the $J_{S\_0–20}$. The E estimates obtained ignoring azimuthal variation were calculated using the J_S from each aspect. Similarly, the error caused by ignoring the tree-to-tree variation was calculated using the J_S from each tree.

In addition, we compared the E_R with the E estimates for multiple sample sizes (n = 1–13), using the same scaling exercise to evaluate the effects of sample size on E estimates. Average E estimates from all possible combinations of sample trees for each sample size were calculated (Kume et al. 2012).

Statistical analysis

The coefficient of variation (CV) for each source of variation was calculated in order to compare the magnitudes of the variations in J_S. All curve fittings were performed with SigmaPlot 10.0 software and were based on the least-squares method (Systat Software, San Jose, CA, USA). Statistical analysis was performed with the SAS version 9.3 software (SAS Institute, Cary, NC, USA).

Results

Spatial variations in J_S

Figure 2 shows the diurnal patterns of J_S (Fig. 2a) and meteorological variables (Fig. 2b) for ten consecutive days from each depth. In general, J_S followed the pattern of Q and D, and J_S showed nocturnal flow while the minimum night D was greater than 0.3 kPa. The average J_S values of $J_{S\_00–20}$, $J_{S\_20–40}$, and $J_{S\_40–60}$ were 10.7, 1.04, and 0.24 g m^{-2} s^{-1}, respectively, indicating that J_S decreased sharply with increasing radial depth. Thus, the radial profile of Korean pine trees showed an exponential decrease with increasing radial depth, and the J_S values had almost

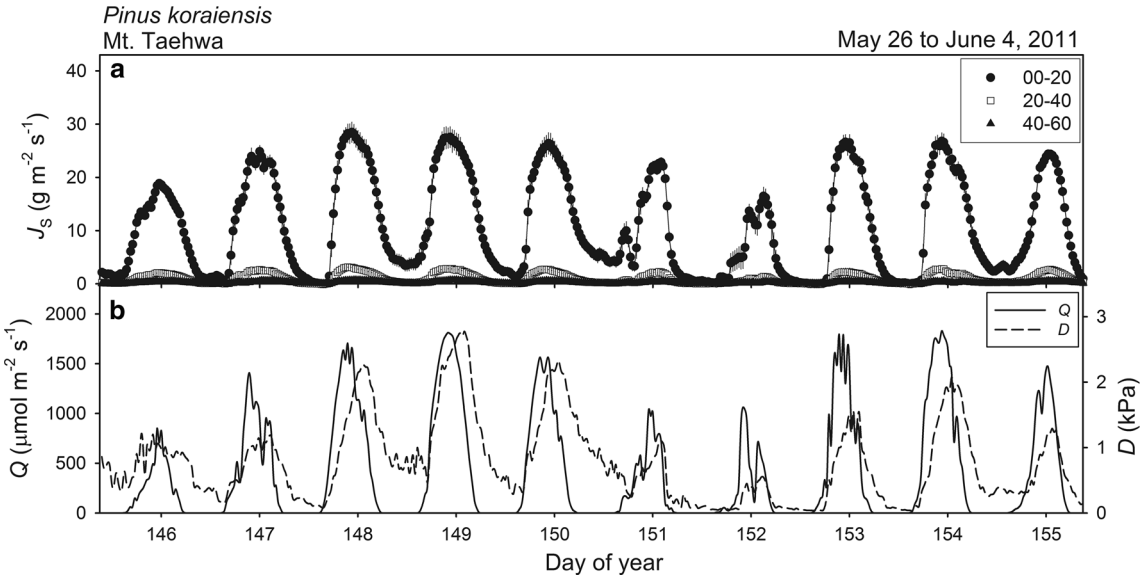

Fig. 2 **a** Diurnal patterns of sap flux densities (J_S) at each depth and **b** meteorological variables (photosynthetically active radiation (Q; *solid line*) and vapor pressure deficit (D; *dashed line*)) during the study period. Each symbol represents a different depth: outermost (0–20; *filled circles*), second (20–40; *open squares*), and innermost (40–60; *filled triangles*). *Error bars* represent the standard error for four trees

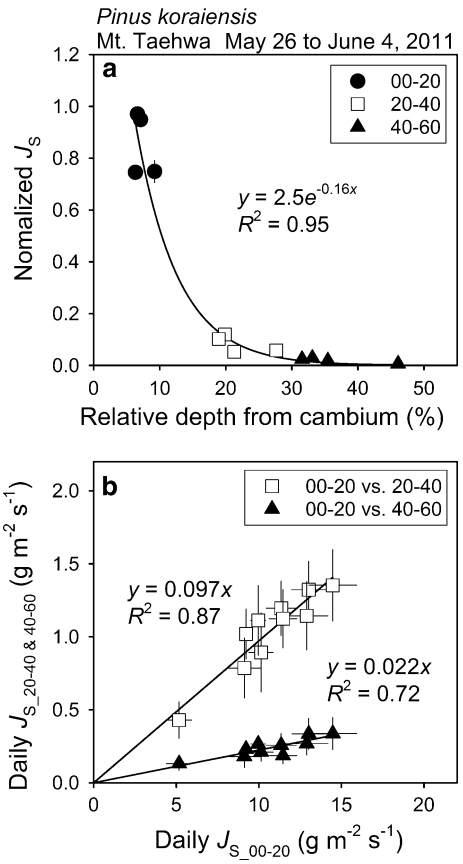

Fig. 3 **a** Radial profile of sap flux density (J_S) and **b** daily average J_S at 0–20 mm ($J_{S\_0\text{-}20}$) vs. 20–40 mm ($J_{S\_20\text{-}40}$) and 0–20 mm ($J_{S\_0\text{-}20}$) vs. 40–60 mm ($J_{S\_40\text{-}60}$). *Symbols* are the same as in Fig. 1. Linear regressions in **b** were forced through the origin. *Error bars* in **a** and **b** represent standard errors for ten days and four trees, respectively

reached zero at approximately 50 % relative depth from the cambium (Fig. 3a). Additionally, the daily average $J_{S\_20\text{–}40}$ and $J_{S\_40\text{–}60}$ values showed linear relationships with $J_{S\_00\text{–}20}$, and the averages of $J_{S\_20\text{–}40}$ and $J_{S\_40\text{–}60}$ were 9.7 and 2.2 % of the average $J_{S\_00\text{–}20}$, respectively (Fig. 3b). These results imply that, in Korean pine trees, the relative contribution from each depth is quite constant and presents substantial radial variation. The average CV of the radial variation for the four trees was 124.3 % (Table 2).

Figure 4a–c show the average diurnal patterns of J_S, and Fig. 4d–f show the average J_S of each aspect for three individual trees during ten days. Although the trends in azimuthal variation were not exactly the same for the individual trees, the J_S values of the eastern aspects were always statistically greater than or equal to those of the western aspects in all three trees (Fig. 4d–f). The average CV of azimuthal variation for the three trees was 23.6 % (Table 2).

Figure 5 shows the J_S diurnal patterns of all fourteen trees during the study period. The average J_S of the fourteen trees was 11.8 g m^{-2} s^{-1}, and the range was 7.0–21.5 g m^{-2} s^{-1}. The J_S variation among the different trees was higher when the J_S values were high, and the CV was correlated with meteorological variables (i.e., CV increased with increasing D), indicating that the differences in the relative contributions of individual trees to the E estimates were greater when D was high (Fig. 6). The CV of the tree-to-tree variation for the fourteen trees was 34.0 % (Table 2).

Sources of error for E estimates

To analyze the error in the E estimates caused by ignoring spatial variation, the differences between the E_R and the E values calculated by ignoring the radial, azimuthal, and tree-to-tree variations were compared (Table 3). On average, the largest error in the E estimates occurred when the radial variation was ignored (109.2 %). Ignoring the azimuthal variation caused the smallest error on average with a normal distribution (12.6 ± 8.4 %). However, E was underestimated by up to 23.6 % when only sensors installed on the southwest aspects of the trees were considered. E was also overestimated by up to 20.3 % when only northeast-aspect sensors were considered. The E estimates from the north-aspect measurements, which are commonly used for J_S measurements to avoid direct solar radiation, had the smallest error (0.6 % compared to the E_R). Ignoring the tree-to-tree variation caused a higher error than ignoring azimuthal variation did, and a lower error than omitting radial variation. The errors also showed normal distributions among the trees, as did the azimuthal variation. The largest error in the E estimates due to ignoring tree-to-tree variation was 65.1 %, and the average error was 24.3 ± 17.9 %.

The effect of sample size on the E estimates compared to the E_R is represented in Fig. 7. The differences in the E estimate (E_D) decreased as the number of samples grew. The average E_D caused by a sample size of 1 was 56.3 ± 45.0 %, and the maximum E_D was 167 %. E_D was <10 % when the sample size was >10.

Discussion

Spatial variations in J_S

The radial profile of J_S usually exhibits the highest rate slightly inside of the cambium and then decreases with increasing radial depth (Nadezhdina et al. 2002; Ford et al. 2004b). However, the shape of this profile varies with species (e.g., Phillips et al. 1996; Jiménez et al. 2000) and sometimes even among individuals of the same species (e.g., Fiora and Cescatti 2006; Poyatos et al. 2007). These different radial profiles could result from factors including

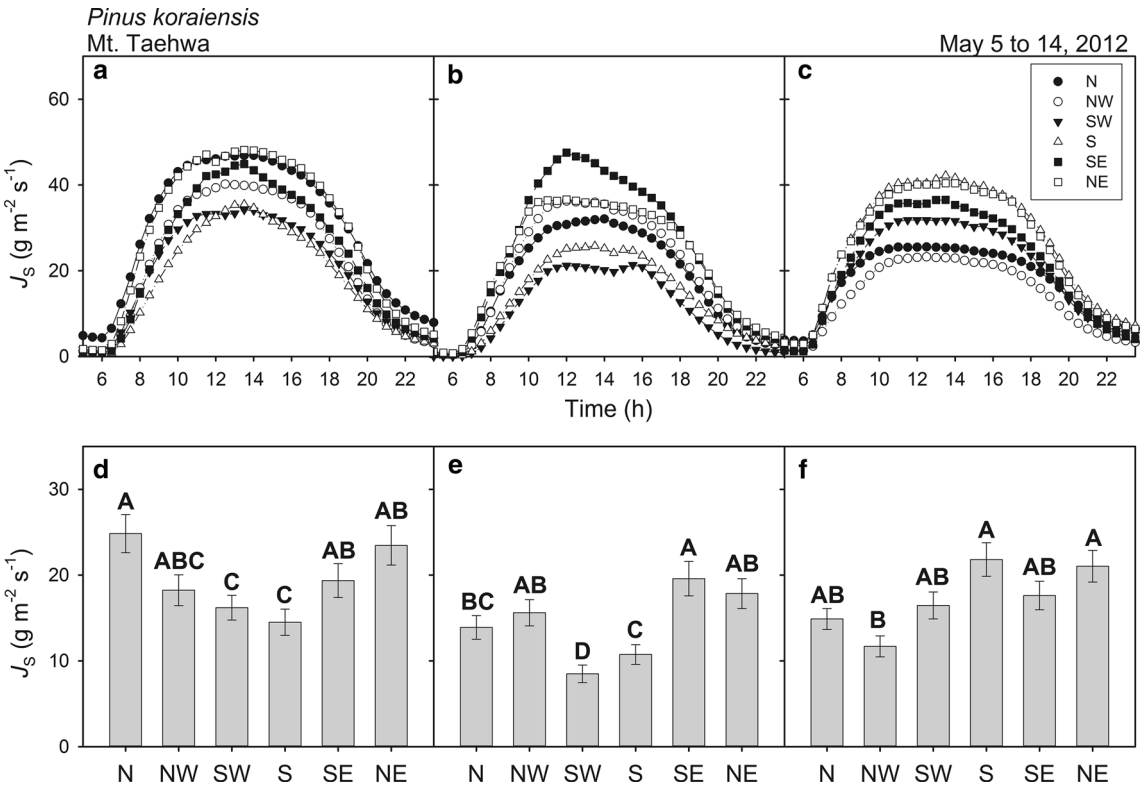

Fig. 4 **a**–**c** Average diurnal patterns of sap flux densities (J_S) and **d**–**f** average J_S from each aspect during the study period (north (N), northwest (NW), southwest (SW), south (S), southeast (SE), and northeast (NE) aspects) in individual trees. **a** and **d**, **b** and **e**, and **c** and **f** represent the sizes of trees in diameter at breast height (26.0, 28.4, and 36.8 cm, respectively). *Different letters* in **d**–**f** indicate differences for which $P < 0.05$. *Error bars* represent the standard error for ten days

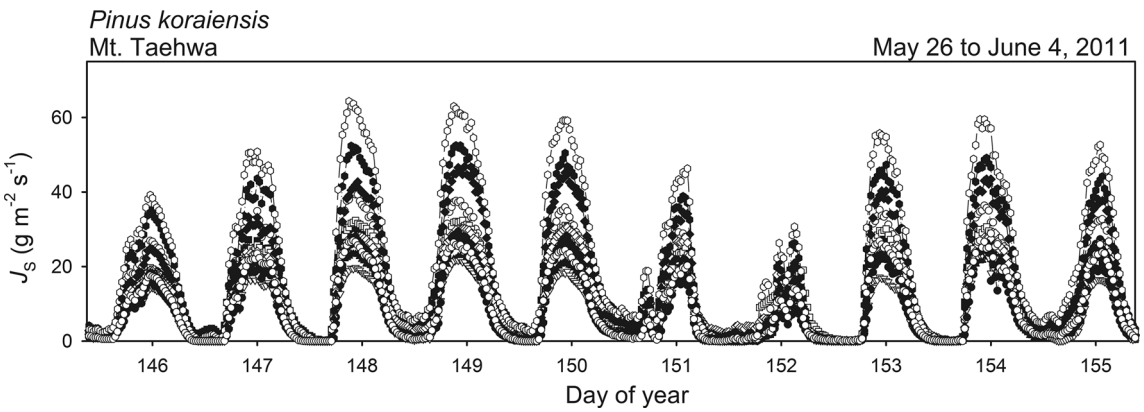

Fig. 5 Diurnal patterns of sap flux densities (J_S) for 14 trees during the study period

the radial variation in the hydraulic conductivity due to differences in tracheid diameter with depth (Tateishi et al. 2008), the proportion of malfunctioning xylem (Paudel et al. 2013), the anatomical connection between the vertical distribution of foliage and the sapwood (Dye et al. 1991), and stand age and tree social position (Fiora and Cescatti 2006). In our study, the average CV of the radial variation was 124.3 % (Table 2), which indicated that transpiration from the outer xylem made a large contribution to J_S when compared to other species (e.g., Phillips et al. 1996; Fiora and Cescatti 2006; Shinohara et al. 2013). In addition, this large contribution of J_S from the outer xylem is species-specific rather than dependent on tree size because the CVs of different size trees will be similar due to the strong relationship between relative depth and normalized J_S (Fig. 3a).

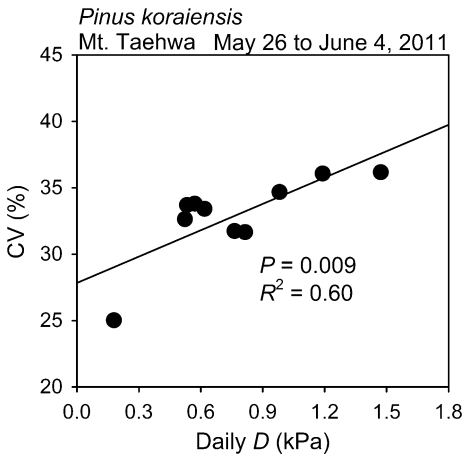

Fig. 6 Relationship between the coefficients of variation (CV) for tree-to-tree variation and daily average vapor pressure deficit (D). Regression line: $y = 6.6x + 27.8$. The data were normally distributed without outliers

Table 3 Differences between the reference stand transpiration (E_R) and the E values calculated by ignoring the radial, azimuthal, and tree-to-tree variations in sap flux densities

Errors	Radial (%)	Azimuthal (%)	Tree-to-tree (%)
Average	109.2	12.6	24.3
Maximum	–	23.6	65.1
Minimum	–	0.6	2.1

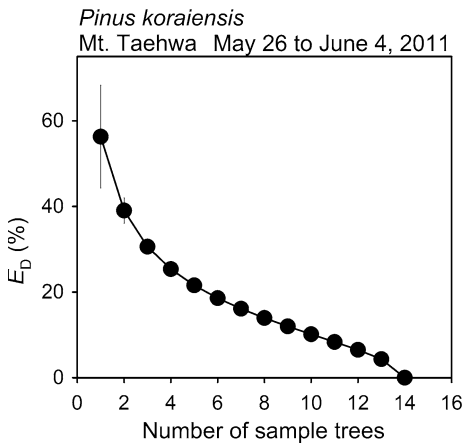

Fig. 7 Effect of increasing the number of sample trees on stand transpiration (E) estimates. The differences in E (E_D) were derived from the differences between the reference E (E_R) and the E derived for each sample size

The azimuthal variation in J_S may result from differences in crown sun exposure (Oren et al. 1999), soil water distribution (Lu et al. 2000), vessel lumen diameter in the xylem (Tateishi et al. 2008), and the direction of the stand side (Shinohara et al. 2013). The smaller J_S associated with the west aspects than with the east aspects in our study may be attributed to our northeast-facing study site, which could have caused large differences in crown sun exposure (Fig. 4). In our study, although the azimuthal variation in J_S was smaller than the other spatial variations, the average CV value of 23.6 % was comparable to those reported for other studies, for which the CV ranges from 21 to 27 % for *Mangifera indica* (Lu et al. 2000), from 15 to 25 % for *Cryptomeria japonica* (Tsuruta et al. 2010), from 23 to 45 % for *Robinia pseudoacacia*, from 22 to 45 % for *Quercus liaotungensis* (Kume et al. 2012), and from 7 to 38 % for *Cryptomeria japonica* (Shinohara et al. 2013).

Tree-to-tree variation may be caused by water-use competition among trees within a stand (Oren et al. 1998; Jimenez et al. 2010). Lagergren and Lindroth (2004) found a correlation between sap flow and competition index that depends on the distance and DBH of neighboring trees, and several studies have reported significant relationships between the water use of trees and tree size (i.e., tree height or DBH) (e.g., Delzon et al. 2004; Shinohara et al. 2013). Although we did not examine the relationship between the water use of an individual tree and its size, our results show that the relative variation in J_S (i.e., CV) among the trees increased with increasing D (Fig. 6). These results indicate that tree-to-tree variation increased with increasing D.

Sources of error in E estimates

In our study, the largest error was caused by radial variation, followed by tree-to-tree and azimuthal variations (Table 3). Kume et al. (2012) and Shinohara et al. (2013) reported that tree-to-tree variation was greater than radial variation in their study sites, although the amount of error caused by ignoring tree-to-tree variation in the present study was comparable to that seen in their results (24 vs. 19–52 %). This difference resulted from the large radial variation in our study, namely, the exponential decrease in J_S with increasing radial depth; however, the related error was well within the range previously reported by other studies (e.g., Nadezhdina et al. 2002; Ford et al. 2004a). In addition, Kume et al. (2012) concluded that azimuthal variation was a minor source of error for E estimates in comparison to other variations, and Shinohara et al. (2013) also reported that the error caused by azimuthal variation was smaller than that of tree-to-tree variation. Our results were in agreement with these findings.

Although greater numbers of sensors provide more accurate E estimates, many studies have been conducted to calculate an ideal minimum sample size in light of limited resources (e.g., Kumagai et al. 2005; Kume et al. 2010b). Similar to the method of Kume et al. (2010b), which determined the minimum sample size with a marginal CV (= dCV/dn) of greater than −0.5, we applied a marginal

error in E estimates (= dE_D/dn) of greater than −0.5 as the minimum sample size. Based on this criterion, the appropriate minimum sample size at our study site was eight, which was similar to the output of the Kume et al. (2010b) method (which ranged from 7 to 9 depending on the simulation). Our minimum sample size created an average 13.9 % error compared to the E_R. Although our minimum sample size is smaller than the 10–15 found by the previous study to be needed for accurate estimations of stand sapwood area and average stand J_S, respectively, in a 20 × 20 m plot, we believe that these differences in minimum sample size can be attributed to differences in stand densities (1,900 vs. 450 trees ha^{-1}). Despite the fact the number was smaller than that recommended by the previous experiment, the ratio of the minimum sample size to the total number of trees was greater in our study (8/20 vs. 15/58), suggesting that the proportion of sample trees needed for accurate E estimates should increase as the total number of trees in a stand decreases.

Conclusions

We examined the radial, azimuthal, and tree-to-tree variations in J_S and their effects on E estimates in a Korean pine stand using Granier-type heat dissipation sensors. Our results clarified the importance of accounting for the spatial variation of J_S, with radial, tree-to-tree, and azimuthal variations being progressively less important. These findings differed from those found in studies by Kume et al. (2012) and Shinohara et al. (2013). Our observations suggest that species- and site-specific consideration of the spatial variation is necessary in order to obtain accurate E estimates—especially the radial variation, which decreased exponentially with increasing radial depth. The azimuthal variation among aspects was significant, but its contribution to the E estimate was minimal in comparison to those of the other variations. Tree-to-tree variation also led to considerable error in the estimated E, and this variation should therefore be accounted for along with the radial variation when attempting to accurately estimate E.

Acknowledgments The primary funding for this study was provided by the Korea Forest Service (project number: S111214L020100) and the Korea Meteorological Administration (project number: 1401-HH-001-02D02-2014). We are also thankful for the support of the Mt. Teahwa Seoul National University Forest and its staff.

References

Alvarado-Barrientos MS, Hernández-Santana V, Asbjornsen H (2013) Variability of the radial profile of sap velocity in *Pinus patula* from contrasting stands within the seasonal cloud forest zone of Veracruz, Mexico. Agric For Meteorol 168:108–119

Barij N, Čermák J, Stokes A (2011) Azimuthal variations in xylem structure and water relations in cork oak (*Quercus suber*). Iawa J 32:25–40

Caylor KK, Dragoni D (2009) Decoupling structural and environmental determinants of sap velocity. Part I. Methodological development. Agric For Meteorol 149:559–569

Cermak J, Nadezhdina N (1998) Sapwood as the scaling parameter defining according to xylem water content or radial pattern of sap flow? Ann For Sci 55:509–521

Čermák J, Kučera J, Nadezhdina N (2004) Sap flow measurements with some thermodynamic methods, flow integration within trees and scaling up from sample trees to entire forest stands. Trees Struct Funct 18:529–546

Chang X, Zhao W, He Z (2014) Radial pattern of sap flow and response to microclimate and soil moisture in Qinghai spruce (*Picea crassifolia*) in the upper Heihe river basin of arid northwestern China. Agric For Meteorol 187:14–21

Clearwater MJ, Meinzer FC, Andrade JL, Goldstein G, Holbrook NM (1999) Potential errors in measurement of nonuniform sap flow using heat dissipation probes. Tree Physiol 19:681–687

Delzon S, Sartore M, Granier A, Loustau D (2004) Radial profiles of sap flow with increasing tree size in maritime pine. Tree Physiol 24:1285–1293

Dye PJ, Olbrich BW, Poulter AG (1991) The influence of growth rings in *Pinus patula* on heat pulse velocity and sap flow measurement. J Exp Bot 42:867–870

Fiora A, Cescatti A (2006) Diurnal and seasonal variability in radial distribution of sap flux density: implications for estimating stand transpiration. Tree Physiol 26:1217–1225

Ford CR, Goranson CE, Mitchell RJ, Will RE, Teskey RO (2004a) Diurnal and seasonal variability in the radial distribution of sap flow: predicting total stem flow in *Pinus taeda* trees. Tree Physiol 24:941–950

Ford CR, McGuire MA, Mitchell RJ, Teskey RO (2004b) Assessing variation in the radial profile of sap flux density in *Pinus* species and its effect on daily water use. Tree Physiol 24:241–249

Ford CR, Hubbard RM, Kloeppel BD, Vose JM (2007) A comparison of sap flux-based evapotranspiration estimates with catchment-scale water balance. Agric For Meteorol 145:176–185

Gebauer T, Horna V, Leuschner C (2008) Variability in radial sap flux density patterns and sapwood area among seven co-occurring temperate broad-leaved tree species. Tree Physiol 28:1821–1830

Granier A (1985) Une nouvelle méthode pour la mesure du flux de sève brute dans le tronc des arbres. Ann For Sci 42:193–200

Granier A (1987) Evaluation of transpiration in a Douglas-fir stand by means of sap flow measurements. Tree Physiol 3:309–320

Granier A, Biron P, Breda N, Pontailler JY, Saugier B (1996) Transpiration of trees and forest stands: short and long-term monitoring using sapflow methods. Glob Chang Biol 2:265–274

Hatton TJ, Moore SJ, Reece PH (1995) Estimating stand transpiration in a *Eucalyptus populnea* woodland with the heat pulse method: measurement errors and sampling strategies. Tree Physiol 15:219–227

Jimenez E, Vega JA, Perez-Gorostiaga P, Fonturbel T, Fernandez C (2010) Evaluation of sap flow density of *Acacia melanoxylon* R. Br. (blackwood) trees in overstocked stands in north-western Iberian Peninsula. Eur J Forest Res 129:61–72

Jiménez MS, Nadezhdina N, Čermák J, Morales D (2000) Radial variation in sap flow in five laurel forest tree species in Tenerife, Canary Islands. Tree Physiol 20:1149–1156

Köstner B, Granier A, Cermák J (1998) Sapflow measurements in forest stands: methods and uncertainties. Ann For Sci 55:13–27

Kubota M, Tenhunen J, Zimmermann R, Schmidt M, Adiku S, Kakubari Y (2005) Influences of environmental factors on the radial profile of sap flux density in *Fagus crenata* growing at different elevations in the Naeba Mountains, Japan. Tree Physiol 25:545–556

Kumagai T, Aoki S, Nagasawa H, Mabuchi T, Kubota K, Inoue S, Utsumi Y, Otsuki K (2005) Effects of tree-to-tree and radial variations on sap flow estimates of transpiration in Japanese cedar. Agric For Meteorol 135:110–116

Kume T, Onozawa Y, Komatsu H, Tsuruta K, Shinohara Y, Umebayashi T, Otsuki K (2010a) Stand-scale transpiration estimates in a Moso bamboo forest. (I) Applicability of sap flux measurements. For Ecol Manage 260:1287–1294

Kume T, Tsuruta K, Komatsu H, Kumagai T, Higashi N, Shinohara Y, Otsuki K (2010b) Effects of sample size on sap flux-based stand-scale transpiration estimates. Tree Physiol 30:129–138

Kume T, Otsuki K, Du S, Yamanaka N, Wang YL, Liu GB (2012) Spatial variation in sap flow velocity in semiarid region trees: its impact on stand-scale transpiration estimates. Hydrol Process 26:1161–1168

Lagergren F, Lindroth A (2004) Variation in sapflow and stem growth in relation to tree size, competition and thinning in a mixed forest of pine and spruce in Sweden. For Ecol Manage 188:51–63

Lu P, Muller WJ, Chacko EK (2000) Spatial variations in xylem sap flux density in the trunk of orchard-grown, mature mango trees under changing soil water conditions. Tree Physiol 20:683–692

Nadezhdina N, Čermák J, Ceulemans R (2002) Radial patterns of sap flow in woody stems of dominant and understory species: scaling errors associated with positioning of sensors. Tree Physiol 22:907–918

Oren R, Phillips N, Katul G, Ewers BE, Pataki DE (1998) Scaling xylem sap flux and soil water balance and calculating variance: a method for partitioning water flux in forests. Ann For Sci 55:191–216

Oren R, Phillips N, Ewers B, Pataki D, Megonigal JP (1999) Sap-flux-scaled transpiration responses to light, vapor pressure deficit, and leaf area reduction in a flooded *Taxodium distichum* forest. Tree Physiol 19:337–347

Paudel I, Kanety T, Cohen S (2013) Inactive xylem can explain differences in calibration factors for thermal dissipation probe sap flow measurements. Tree Physiol 33:986–1001

Phillips N, Oren R, Zimmermann R (1996) Radial patterns of xylem sap flow in non-, diffuse-and ring-porous tree species. Plant Cell Environ 19:983–990

Poyatos R, Čermák J, Llorens P (2007) Variation in the radial patterns of sap flux density in pubescent oak (*Quercus pubescens*) and its implications for tree and stand transpiration measurements. Tree Physiol 27:537–548

Ryu D, Moon M, Park J, Cho S, Kim T, Kim HS (2014) Development of allometric equations for V age-class *Pinus koraiensis* in Mt. Taehwa plantation Gyeonggi-do. Kor J Agric For Meteorol 16:29–38

Shinohara Y, Tsuruta K, Ogura A, Noto F, Komatsu H, Otsuki K, Maruyama T (2013) Azimuthal and radial variations in sap flux density and effects on stand-scale transpiration estimates in a Japanese cedar forest. Tree Physiol 33:550–558

Tateishi M, Kumagai T, Utsumi Y, Umebayasi T, Shiiba Y, Inoue K, Kaji K, Cho K, Otsuki K (2008) Spatial variations in xylem sap flux density in evergreen oak trees with radial-porous wood: comparisons with anatomical observations. Trees Struct Funct 22:23–30

Tsuruta K, Kume T, Komatsu H, Higashi N, Umebayashi T, Kumagai T, Otsuki K (2010) Azimuthal variations of sap flux density within Japanese cypress xylem trunks and their effects on tree transpiration estimates. J For Res 15:398–403

Wilson KB, Hanson PJ, Mulholland PJ, Baldocchi DD, Wullschleger SD (2001) A comparison of methods for determining forest evapotranspiration and its components: sap-flow, soil water budget, eddy covariance and catchment water balance. Agric For Meteorol 106:153–168